Lifetime of Objects in Geostationary Transfer Orbit

G. Janin

Mission Analysis Section
European Space Operations Centre, 6100 Darmstadt, FRG

Abstract

Objects in Geostationary Transfer Orbit (GTO) result from the launch of satellites in geostationary orbit. There are actually close to 200 GTO objects, most of them are third-stage rockets used for transferring satellites from low Earth orbit to geostationary orbit. By crossing the low Earth orbits region at high speed more than twice a day, they represent a hazard for low Earth orbiting satellites. This paper intents to

1. *describe the situation in GTO and stress the danger presented by these objects for the low Earth satellite population,*
2. *indicate the source and accuracy of tracking data,*
3. *recall the effect of orbital perturbations on the orbit evolution,*
4. *outline first attempts to determine ballistic coefficients,*
5. *discuss the accuracy of re-entry prediction,*
6. *give the range of expected lifetimes.*

1. Introduction

Due to its unique coverage property from a ground station, the geostationary orbit is the preferred location for application satellites. More than 250 satellites, active or defunct, are actually cruising in or around the geostationary orbit.

The geostationary orbit is reached via a Geostationary Transfer Orbit (GTO), which allows to connect the near-Earth environment to the geostationary radius at 35786 km altitude (Fig. 1).

A typical GTO with a perigee height of 200 km has the following orbital parameters:

- semi-major-axis: 24371 km
- eccentricity: 0.73
- argument of perigee: 180°
- orbital period: 10.52 h

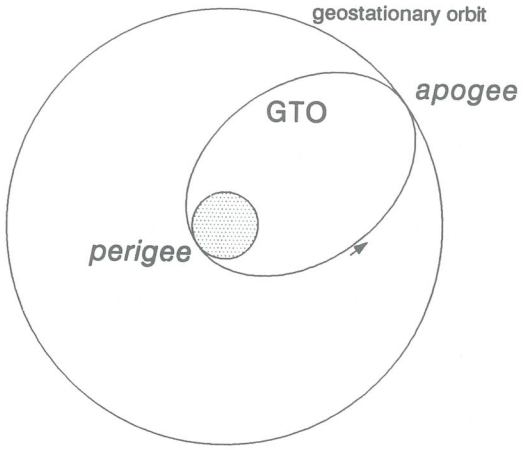

Figure 1. Geostationary Transfer Orbit: perigee height: 200 km, vanishes on this scale.

The orbital inclination depends on the latitude of the launch site and is between 5° and 10° for an ARIANE launch from Kourou.

In most of the cases, the launcher delivers the satellite on the GTO and an additional motor, attached to the satellite, propulses it on the geostationary orbit, at the apogee of the GTO. This means that the upper stage of the launcher stays on the GTO. It will therefore cross through the low Earth satellite population more than twice a day with a relative velocity from 3 to 12 km/s depending on the relative inclination of the orbital planes. How many of these objects are revolving on the GTO and how long do they stay there ?

This paper will attempt to give an answer to these questions.

2. The Situation in GTO

Almost all objects in GTO are passive and abandoned. Passive means that their on-board transponder is inoperative and insensible to any commands. These objects are abandoned and there is little concern of what happened to them.

Proc. Internat. Workshop on Salyut-7 / Kosmos-1686 Reentry, ESOC, Darmstadt (D), 9 April 1991

However, in their effort of monitoring all sizable objects revolving around the Earth, the US Space Command does include objects in GTO into their catalogue. This catalogue, containing orbital elements of objects of size larger than 10 cm, is obtained by radar tracking or optical observations.

The following section will show that objects initially on GTO have their orbit changed under the effect of orbital perturbations. Therefore, actual GTO objects do not necessarily possess strict GTO elements. In order to collect most of the GTO objects, a count of all catalogued objects whose perigee height is below 500 km and apogee height between 10000 and 40000 km was undertaken. For March 1991, there are 187 such objects.

If only GTO objects under ESA's responsibility are taken into consideration, Table 1, compiled from Ref. 1., lists the total number of objects catalogued, still in orbit or decayed. Objects, which are not third-stages or multiple launch structures are capsules, adapters or radio amateur satellites. Rocket third-stages form the major part of the ESA GTO population, and such a conclusion is also expected for the total GTO population.

	Total	3rd-stages	MLS
Catalogued	30	17	11
Flying	17	14	2
Decayed	13	3	9

Table 1. Situation of catalogued ESA/ESRO objects in GTO: Status on April 1991. MLS is an acronym for ARIANE Multiple Launch Structure, such as Sylda or Spelda.

3. Perturbations of GTO

3.1 Third-body Perturbation

The third-body perturbation is dominating the behaviour of highly eccentric orbits. It is due to the gravitational influence of the Sun and the Moon and is characterised by:

1. little or no effect on the semi-major axis,
2. a fluctuation of the eccentricity of long period due to the Sun and of short period due to the Moon,
3. a small variation of the angular elements.

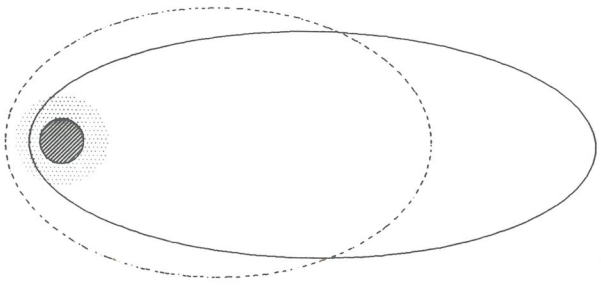

Figure 2. Third-body perturbation on a highly eccentric orbit: The third-body perturbation changes the orbital eccentricity. A reduction of the eccentricity (circularisation) is shown here.

The fluctuation in eccentricity translates into a variation of the perigee height and a corresponding opposite variation of the apogee height (Fig. 2).

An approximated expression of the rate of change for the orbital elements can be obtained by expanding the disturbing force in power of the ratio of the orbital radius vector over the third-body radius vector in the Lagrange planetary equations. The long-term behaviour can be estimated by considering only the first order terms and by averaging the equations over one revolution of the satellite while keeping the position of the third-body fixed. By a second averaging, this time over one revolution of the third-body supposed to be on a circular orbit of radius r_1, the following result is obtained for the variation of the perigee radius δr_p (Ref. 2.):

$$\delta r_p = -\frac{15}{4}\pi\frac{\mu_1}{\mu}\left(\frac{a}{r_1}\right)^3 ae\sqrt{1-e^2}\,\sin^2 i \sin 2\omega$$

where μ_1/μ is the ratio of the gravitational constant of the third-body to the central body. The sign of the variation of the perigee height depends therefore on the quadrant in which the perigee is located. When the perigee is in the first or third quadrant its height decreases and may lead to orbital decay.

Due to the rotation of the argument of perigee induced by the oblatenes perturbation, the overall behaviour of the perigee height during a long period cannot be simply predicted.

On a GTO, the perturbation by the Moon is of small magnitude and the perturbation by the Sun leads to a perigee height oscillation of $\pm$50 km mean amplitude with maximum peaks of $\pm$75 km and a period of about 9 months.

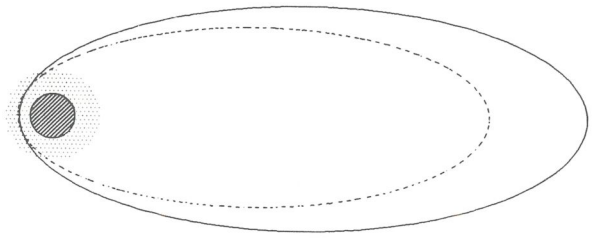

Figure 3. Atmospheric drag perturbation on a highly eccentric orbit: The drag perturbation acts at perigee and reduces the apogee height.

3.2 Atmospheric Drag Perturbation

GTO objects are injected with a perigee at relatively low altitude (typically 200 km). Even if luni-solar perturba-

tions raise this altitude by 50 to 75 km, the GTO perigee is still inside the atmosphere and subjected to drag perturbation. This perturbation decreases the orbital energy, therefore the semi-major-axis. The perigee height is not affected, but the apogee height is decreased by a small distance at each revolution (Fig. 3).

3.3 Combined Effect of Third-body and Drag Perturbations

The apogee height decrease caused by atmospheric drag at perigee reduces the luni-solar effect. Therefore, the perigee height motion is damped. If for instance the perigee height was to decrease by a specific distance due to the luni-solar perturbation, it will actually decrease by a smaller distance. This may paradoxically *extend* the lifetime of the satellite. Here is an example of drag perturbation helping to delay the decay of a satellite.

In conclusion, the combined effect of third-body perturbation and atmospheric drag makes orbital evolution prediction hazardous, more hazardous than in the case of a near-Earth satellite subjected only to drag.

4. Estimation of the Ballistic Coefficient

The atmospheric drag perturbation force on the orbit is proportional to

$$1/2 c_D S/m,$$

where c_D is the *drag coefficient*, S the cross sectional area and m the mass of the satellite. This expression is called *ballistic coefficient*. The drag perturbation force is obtained by multiplying the ballistic coefficient by the local air density ρ and the square of the spacecraft velocity relative to the atmosphere.

Poorly known is the drag coefficient, depending on the shape and surface of the satellite, the cross sectional area, depending on the satellite's attitude, and the air density, depending on the altitude, Sun's direction and activity. In Ref. 3., the dependence of the drag coefficient with the velocity incidence angle α (angle between the spacraft's main axis and the velocity vector) for ARIANE third stages, with and without upper multi-launch structure, is investigated (Fig. 4).

In the case of an uncontrolled spacecraft, its attitude is unknown. The only hope on obtaining orientation information is by dedicated visual or radar observation. Up to now, no such observation is available for GTO objects, therefore, only a guess value for the mean cross sectional area can be given.

The uncertainty in the knowledge of the air density is a well known problem for decay prediction of near-Earth satellites on near-circular orbits. Satellites on GTO are also subjected to this uncertainty.

By taking a mean cross-sectional area applied to observed ARIANE 4 third-stage trajectories, using a parameter estimation method a comparison was made with the theoretical drag coefficient values computed in Ref. 3. It turned out that the obtained drag coefficient was about two times higher than the range of theoretical values (Fig. 5).

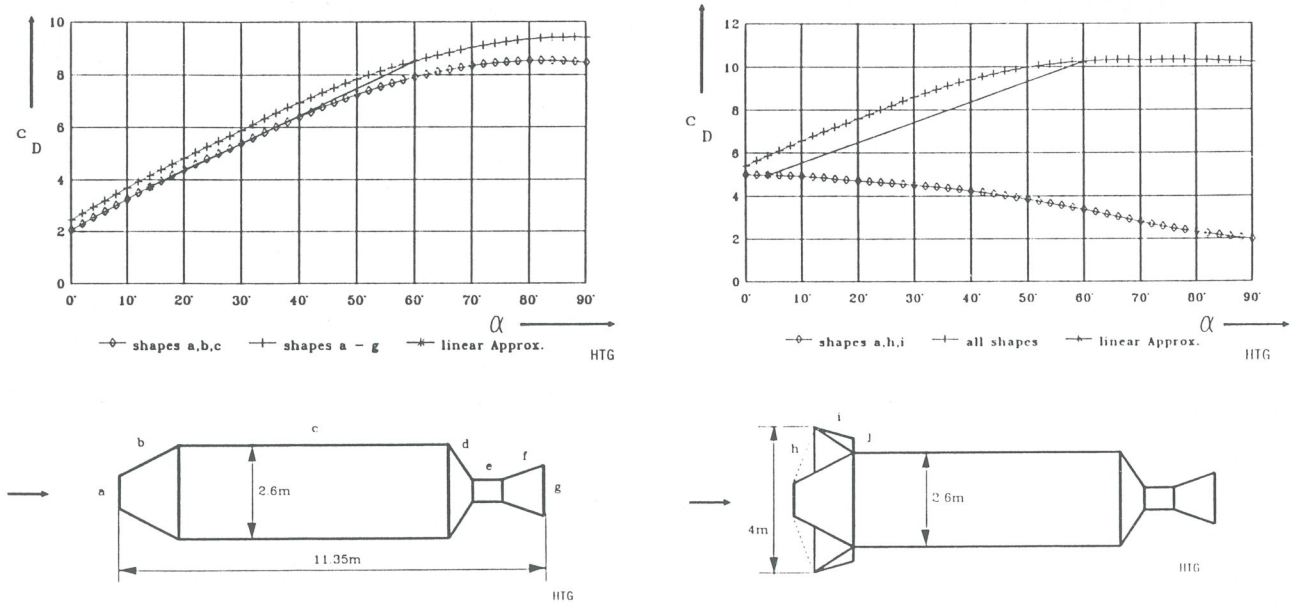

Figure 4. ARIANE 4 third-stage: Estimation of the drag coefficient for the ARIANE 4 third-stage by shape element method using Pike's theory (Ref. 3.) in terms of the flight attitude α with the relative velocity vector. The right hand side Fig. treats the case when the lower multiple launch structure SPELDA is on top of the third stage. The shadowing of some shape elements (a, b, c, ...) among themselves needs the consideration of two separate cases, which can be related by a linear approximation curve (Fig. courtesy of Hyperschall Technologie Goettingen).

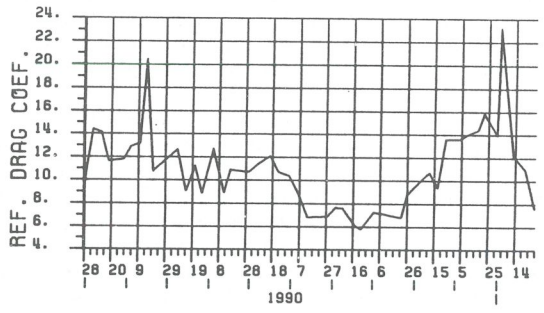

Figure 5. Drag coefficient estimation from observations: Parameter estimation method applied to TLE resulting from the tracking of ARIANE flight V29 third-stage (1989-020 C) between 90-03-06 and 91-01-25.

This disappointing result, contrasting with good results such an approach has shown for low-Earth near circular orbits, is most certainly due to

1. too crude consideration on the choice of the cross sectional area,
2. uncertainty in the air density,
3. large uncertainty of about ± 8 km in the actual perigee height.

Point 3 results from the analysis of US Space Command data (see below Section 5.3).

5. Lifetime Estimation

An estimation of the orbital lifetime of a satellite is obtained by propagating the orbit until the perigee is in the dense atmosphere. Capabilities of analytical theories are poor for third-body perturbations estimation, therefore one has to resort to semi-analytical or numerical methods for GTO accurate propagation.

5.1 Semi-analytic Methods

Most semi-analytical methods are based on averaged orbital elements. They perform well but the conversion from osculating to averaged elements and vice versa is usually poorly defined. Observed state vectors result in osculating elements, therefore there is all the time a doubt that the semi-analytical method based on averaged elements integrates an orbit, which initial state is slightly off the input one.

This problem is absent in the *stroboscopic method* developed by E. A. Roth (Ref. 4.). In this method, orbital perturbations are integrated analytically along one revolution on the basis of the initial osculatory state at a particular reference point on the orbit (perigee, node, etc.). This procedure is then repeated for many revolutions. Since the orbital state is provided only once per revolution, a stroboscopic view of the trajectory is obtained.

5.2 Numerical Integration

Numerical schemes for orbit propagation allow using perturbation models as realistic as needed. The accuracy of the integration is limited only by computing power. A numerical orbit propagation method consists of:

1. a formulation of the differential equations of the motion (i. e. Newton's equations, time transformation, use of a time element, regularised variables, orbital elements, uniformly regular elements, etc.);
2. an integration scheme (single-step, multi-step, multi-revolution, etc.);
3. a perturbation model.

with the help of the tool USOC (Unified System for Orbit Computation, see Ref. 5.), an efficient program was built for the particular case of GTO. As moderate accuracy long-term propagation would be accomplished with a semi-analytical method, this program aims at high accuracy for short term orbit propagation.

The trajectory computation is divided in two phases. The following numerical components are chosen:

- Phase 1, propagation under luni-solar and drag perturbation:
  1. as high accuracy is desired for relatively short term orbit propagation (a few hundred of revolutions) a formulation in terms of orbital elements is not necessary and differential equations in Cartesian coordinates are taken. However, as the orbit is eccentric, a transformation of the independent variable in true anomaly, giving the highest density of integration steps around perigee, is chosen. In order to have a good estimation of the time, a time element is added. Such a formulation is discussed in Ref. 6.
  2. As many revolutions have to be integrated, an efficient 8th order multistep integrator is chosen with a corresponding 8th order Runge-Kutta method as a starter.
  3. The air density model is a Jacchia-Lineberry model, depending on the mean and daily 10.7 cm solar activity flux and geomagnetic index. This density model offers high accuracy while keeping computation overhead at a reasonable level. The solar activity parameters are taken out of a table of actual or predicted values.
  4. For the potential of the Earth, only the J_2 term is taken, the higher terms do not play a significant role for orbital decay studies.
- Phase 2, the final revolutions with vanishing third-body perturbation and heavy atmospheric drag:
  1. As the orbit is still eccentric, the same formulation as in Phase 1 is chosen, however without the time element.
  2. As the atmospheric drag perturbation can have an extremely high magnitude, larger than the central body attraction, the fixed step size integration has to be substituted by a more flexible integration with adaptive step

size regulation: a Runge-Kutta-Fehlberg 7/8 method is chosen.

3. The air density model is extended toward the Earth surface until altitude zero by an exponential model.

5.3 Initial Values

Initial values for decay prediction of passive objects are hard to obtain. For GTO objects, the only regular source of orbital elements is the US Space Command catalogue of space objects. This catalogue is composed of so-called *Two-Line Elements* (TLE), resulting mostly from radar observations. The TLE, distributed by NASA, are quadruply averaged elements (averaged in 1/ true anomaly, 2/ argument of perigee, 3/ the motion of the Sun, 4/ the motion of the Moon), as defined by the SDP-4 theory used at US Space Command for objects in highly eccentric orbits. TLE are given at the orbital ascending node and the corresponding transformation into osculating elements is provided. No accuracy is given for these TLE.

In order to have an idea on the accuracy of TLE of GTO objects, a series of comparisons was made between a sequence of TLE observations and a corresponding numerical integration for given objects. The initial state and the drag coefficient for the numerical integration was obtained from TLE with the parameter estimation mentioned in Chap. 4. This method, as said in Chap. 4, is not very satisfactory and leads to initial elements possibly apart from the real ones. However, the behaviour of the TLE orbit and the numerically integrated one should be similar, especially the variation pattern of the perigee height. It is not, as Fig. 6 (TLE orbit versus numerically integrated orbit) show.

The numerical integration scheme has been applied many times to real cases of operated satellites and has proved to be reliable. It is therefore clear that the irregular perigee height behaviour exhibited in the TLE orbit is not a real behaviour but rather the result of dispersions in the TLE. By inspecting Fig. 6, dispersion of up to 10 km can be noticed. This is a scale of the uncertainty of the TLE for GTO.

5.4 Results

After each launch of a new spacecraft, the Royal Aerospace Establishment estimates the orbital lifetime of the satellites and rocket stages associated with the launch. These lifetimes are compiled into the RAE Table of Satellites (Ref. 7.). For those objects on highly eccentric orbits, which inclination does not vary too much during the lifetime, an analytical/graphical method has been designed by Walker & King-Hele (Ref. 8.). The method consists of decoupling the third-body from drag perturbation. Orbit evolution under drag, even for eccentric orbits, can be estimated analytically and represented in a graphical form in terms of perigee height, eccentricity and ballistic parameter. Concerning third-body perturbation, only the effect on the perigee height is taken into account. This can be analytically estimated with the help of a formula of the type proposed in Section 3.1, which can be used for defining a mean perigee height. This mean perigee height is then used in the graphics to read the life time.

This method has proved to be quite reliable for GTO. The obtained range of predicted lifetimes is very large: from 0 day (case of ARIANE flight V20 on 87-11-21 where the third-stage '1987-95 B' re-entered the same day) to more than 5000 years.

Initial lifetime estimation performed shortly after launch are based on orbital initial values obtained from orbit determination. These orbital elements, resulting from the tracking of spacecraft still active, are more accurate than TLE. This leads to the paradox that a life time estimation performed recently (based on TLE) may be less accurate than the initial one made immediately after launch.

In Ref. 9., a typical example of the accuracy to expect for GTO objects lifetime estimation is given. The object is 1979-104 A (CAT-1, Capsule Ariane Technologique 1), payload of the first Ariane launch, orbited on December 24, 1979. CAT-1 is composed of a 217 kg technological capsule and a 1385 kg ballast. The mean cross sectional area is about 1.5 square meter.

The initial RAE lifetime estimation was 10 years (Ref. 7.), which means a re-entry on December 1989.

Indeed, CAT-1 re-entered on November 27, 1989. The initial RAE prediction was extremely good.

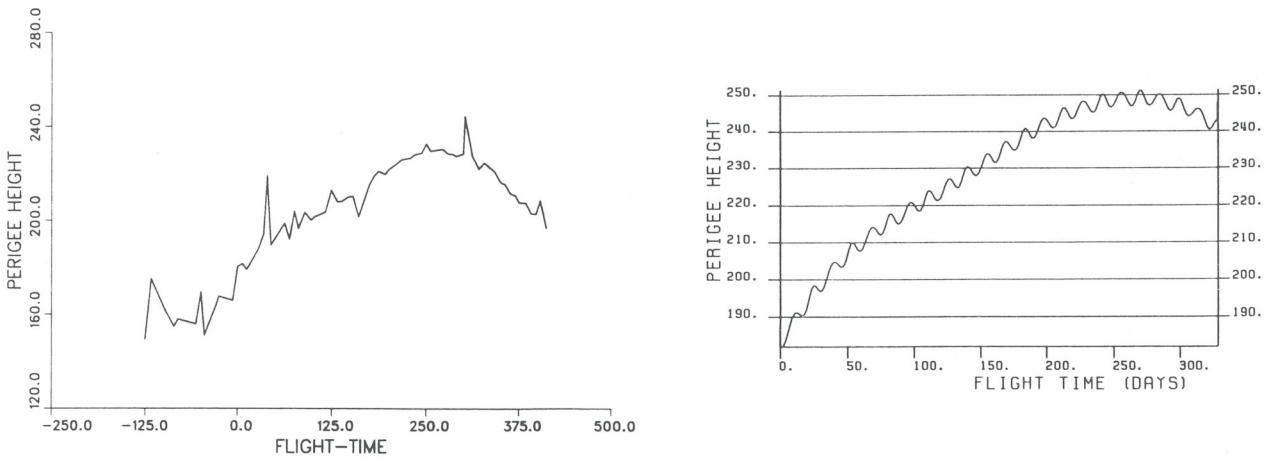

Figure 6. ARIANE 4 flight V29: Third-stage (1989-20 C) perigee height history according to Two-Line Elements (left hand side Fig.) and numerical integration (right hand side Fig.) during 90-03-06 to 91-01-25.

However, a RAE prediction made only 7 weeks before re-entry forecasted the decay on December 20, 1989. This was in error by 40 %, illustrating the paradox mentioned above.

Since 1985, for objects whose lifetime is shorter than 10 years, ESOC predicts the re-entry of ESA objects and Ariane launches (Ref. 10.). These predictions, performed in the case of GTO objects with the stroboscopic method and based on most current TLE, are included in the *ESA Bulletin of Space Objects* (Ref. 1.). This bulletin is produced by the Mission Analysis Section of ESOC and distributed several times per year. The history of the corresponding CAT-1 decay predictions is graphically represented on Fig. 7 as a function of the date when the prediction was made.

Figure 7. History of the ESOC decay prediction of CAT-1: Capsule Ariane Technologique 1 (1979-104 A), payload of the first ARIANE flight.

Fig. 7 shows the considerable dispersion of the predictions. It shows also that the dispersion does not reduce significantly toward the end of the lifetime. For instance, on 89-10-04 the decay was still predicted for August 1990, in error of 8 months from the actual date, and this only two months before actual re-entry. As explained in Ref. 9., this large dispersion is mostly due to the uncertainty of the TLE.

An analysis of the computer runs made for decay prediction showed that by moving the perigee height resulting from the TLE by a distance of the order of ± 10 km, the actual re-entry date could be reproduced (Ref. 9.). This confirms the uncertainty of the TLE for GTO.

6. Conclusion

Lifetime of GTO objects can extend from an immediate re-entry to more than 5000 years into orbit. Lifetime prediction is subjected to numerous uncertainties:

- the perigee height is oscillating with an irregular amplitude of ± 50 km average due to luni-solar perturbations,
- the drag perturbation, operating at perigee, is subjected to an uncertainty due to the inaccurate knowledge of the atmospheric density,
- the cross-sectional area of the object, which in case of a rocket third-stage is usually an elongated cylinder, is poorly known due to the absence of observation on the attitude motion,
- the only regular source of information on orbital debris elements are the NASA TLE. They are found to be of insufficient accuracy (± 10 km on the perigee height for GTO).

This renders the lifetime prediction of GTO objects hazardous, even if state-of-the-art orbit propagation methods are used.

References

1. ESA Bulletin of Space Objects, ESA/ESOC, Mission Analysis Section (latest issue: May 1991).
2. Roth E A 1974, Evolution of the Transfer Orbit to the Synchronous Height and Preliminary Launch Window Study for the Passenger Satellite of the Ariane Vehicle, *ESOC Internal Note* **156**, ESA/ESOC.
3. Determination of Spacecraft Parameters Using Radar Data, *ESA Contract No. 8424/89/D/MD*, ESA/ESOC (1991).
4. Roth E A 1977, Mission Analysis for Terrestrial Satellite and Planetary Orbiters, with Special Emphasis on Highly Eccentric Orbits: 1. The Mathematical Background, *ESA Jour.* Vol 1, 245-268.
5. Janin G 1978, Mission Analysis for Terrestrial Satellite and Planetary Orbiters, with Special Emphasis on Highly Eccentric Orbits: 2. The Software Design, *ESA Jour.* Vol. 2, 201-206.
6. Janin G & Bond V R 1981, A General Time Element for Orbit Integration in Cartesian Coordinates, *Adv. Space Res.* Vol. 1, No. 6, 69-78.
7. King-Hele D G, Walker D M C, Winterbottom A N, Pilkington J A, Hiller H & Perry G E 1990, The RAE Table of Earth Satellites 1957-1989, RAE, Farnborough.
8. Walker D M C & King-Hele D G 1986, Lifetime Predictions for the RAE Table of Satellites, *ESA SP-246*, 29-38.
9. Janin G 1991, Decay of Debris in Geostationary Transfer Orbit, *Adv. Space Res.* Vol. 11, No. 6, (6)161-(6)166.
10. Janin G & de Leeuw J 1986, Decay of ESA Space Objects, *ESA SP-246*, 75-80.